

Phenomenology of collinear photon emission from quark-gluon plasma in AA collisions

B.G. Zakharov¹

¹*L.D. Landau Institute for Theoretical Physics, GSP-1, 117940, Kosygina Str. 2, 117334 Moscow, Russia*

(Dated: March 25, 2022)

We study the role of running coupling and the effect of variation of the thermal quark mass on contribution of the collinear bremsstrahlung and annihilation to photon emission in AA collisions in a scheme similar to that used in our previous jet quenching analyses. We find that for a scenario with the thermal quark mass $m_q \sim 50 - 100$ MeV contribution of the higher order collinear processes summed with the $2 \rightarrow 2$ processes can explain a considerable part ($\sim 50\%$) of the experimental photon spectrum at $k_T \sim 2 - 3$ GeV for Au+Au collisions at $\sqrt{s} = 0.2$ TeV. But for $m_q = 300$ MeV and for the thermal quark mass predicted by the HTL scheme the theoretical predictions underestimate considerably the experimental spectrum.

PACS numbers:

I. INTRODUCTION

The observation of jet quenching phenomenon and hydrodynamical flow effects in AA collisions at RHIC and LHC signals about formation of a hot quark-gluon plasma (QGP) in the initial stage of AA collisions. It seems likely that the QGP formation goes via the thermalization of the collective color fields of the so-called glasma stage [1, 2] formed after multiple gluon exchanges between two strongly Lorentz contracted nucleus disks. It is believed that the QGP should also reveal itself in thermal photon emission that may be important in the low and intermediate k_T region [3]. However, the photon production in AA collisions shows some inconsistency with the QGP evolution supported by the results of the jet quenching analyses. The data from RHIC and LHC on jet quenching in AA collisions can be explained in the picture with radiative and collisional energy loss for the hydrodynamical QGP evolution with the QGP production time $\tau_0 \sim 0.5$ fm and the initial entropy determined from the measured hadron multiplicities [4–6]. However, theoretical predictions for the thermal photon spectrum in this picture obtained with a sophisticated viscous hydrodynamical model of the fireball evolution [7] underestimate the photon spectrum measured at RHIC by PHENIX [8] in Au+Au collisions at $\sqrt{s} = 0.2$ TeV by a factor of ~ 3 . Several mechanisms have been suggested that can increase the photon emission in AA collisions. There were suggestions that very strong magnetic field created in noncentral AA collisions can increase the photon emission due to the conformal anomaly [9] and the synchrotron radiation [10]. However, these mechanisms require too high magnitude of the magnetic field [11], that contradicts to calculations for realistic evolution of the plasma fireball [12]. In Ref. [13] it was suggested that a considerable additional contribution to the photon production may be due to the boundary bremsstrahlung resulting from interaction of escaping quarks with collective confining color field at the surface of the QGP. In Refs. [14–16] it was argued that the pre-equilibrium glasma phase also can give large contribution to the photon emission in AA collisions. Unfortunately, uncertainties in the

theoretical predictions for the boundary photon emission [13] and the photon emission from the glasma [14–16] are rather large.

As compared to the glasma stage the photon production in the QGP stage is better understood. However, even for the QGP phase the theoretical uncertainties can be considerable, because the available analyses are based on the pQCD picture of a weakly coupled QGP. And its applicability to the QGP produced at RHIC and LHC may be questionable. In the leading order (LO) pQCD the thermal photon emission from the QGP is due to the $2 \rightarrow 2$ processes: $q(\bar{q})g \rightarrow \gamma q(\bar{q})$ (Compton) and $q\bar{q} \rightarrow \gamma g$ (annihilation). In the pQCD picture a significant contribution to the photon emission comes also from the higher order collinear processes $q \rightarrow \gamma q$ and $q\bar{q} \rightarrow \gamma$ [17]. It turns out to be parametrically of the same order as the $2 \rightarrow 2$ processes [18]. The results of Ref. [17] show that at $k/T \gtrsim 3$ contribution of the collinear processes turns out to be close to that from the LO $2 \rightarrow 2$ mechanisms, and at $k/T \lesssim 2$ the collinear emission gives the dominant contribution to the photon emission rate in the QGP. The collinear photon radiation is due to multiple scattering of thermal quarks in the QGP. This mechanism is similar to that for the photon radiation from hard quarks [19] and to the induced gluon radiation from fast partons that dominates in the jet quenching phenomenon [20–23]. In [17] the collinear processes have been evaluated for constant QCD coupling using the thermal field theory methods within the hard thermal loop (HTL) resummation scheme. In the case of the induced gluon emission from fast partons in the QGP the results for constant and running α_s differ considerably. For running α_s the energy dependence of the radiative parton energy loss weakens [24]. The analyses of the data on the nuclear modification factor R_{AA} from RHIC and LHC [6, 24, 25] show that running α_s allows to obtain a better agreement with the data. In [7] the photon emission has been addressed using the AMY [17] formulas obtained for a fixed QCD coupling constant. For accurate confronting the QGP signals from jet quenching and from photon production it would be of great interest to perform calculations of the collinear photon emission with running α_s consistent

with that used in the successful jet quenching analyses. Also it would be interesting to study the sensitivity of the collinear photon emission to variation of the quark quasiparticle mass m_q . The predictions of the pQCD analysis [17], based on the HTL resummation scheme, have been obtained for the standard pQCD quark quasiparticle mass $m_q = gT/\sqrt{3}$. However, the analysis of the lattice data within a quasiparticle model [26] gives practically constant thermal quark mass $m_q \sim 300$ MeV. In a more recent analysis [27] it was demonstrated that in a strongly coupled QGP the thermal quark mass may be much smaller than that in the pQCD HTL picture. A two-pole fit (with the normal and plasmino modes) of the Euclidean lattice quark correlator of Ref. [28] also supports that the thermal quark mass may be smaller than in the HTL scheme (by a factor of ~ 2). However, unfortunately the fit is not very accurate due to the insensitivity of the Euclidean correlator to the quark spectral function at energies $\lesssim T$ [28]. The small thermal quark mass may increase the photon emission rate, with a very small effect on the jet quenching that is practically insensitive to the quark quasiparticle mass [21, 22]. Due to the theoretical uncertainties for the thermal quark mass, it would be interesting to study the collinear photon emission in a phenomenological picture without the HTL constraints on the quark quasiparticle mass.

In the present paper we study the effect of running α_s and the role of variation of the quark quasiparticle mass on the collinear photon emission in AA collisions. We treat quark multiple scattering in the QGP in the scheme we used previously in successful jet quenching analyses [4, 25]. There we used the Debye mass obtained in the lattice calculations that, contrary to the HTL scheme, give nonzero magnetic screening [29] in the QGP. We compare the results for this scenario with the results for the HTL scheme with static α_s . We use the formalism of [30] based on the light-cone path integral (LCPI) approach [22, 23]. The formulation given in [30] reproduces the results of the AMY [17] approach. In [17] the photon emission rate has been expressed via solution of an integral equation. In the present paper the photon emission rate is expressed via solution of a two-dimensional Schrödinger equation with a smooth boundary condition. The method is convenient for numerical calculations.

II. THEORETICAL FRAMEWORK

The contribution of the collinear processes $q \rightarrow \gamma q$ and $q\bar{q} \rightarrow \gamma$ to the photon emission rate per unit time and volume in the plasma rest frame can be written as [17, 30]

$$\frac{dN}{dtdVd\mathbf{k}} = \frac{dN_{br}}{dtdVd\mathbf{k}} + \frac{dN_{an}}{dtdVd\mathbf{k}}, \quad (1)$$

where the first term corresponds to $q \rightarrow \gamma q$ and the second one to $q\bar{q} \rightarrow \gamma$. The bremsstrahlung contribution can be written as [30]

$$\frac{dN_{br}}{dtdVd\mathbf{k}} = \frac{d_{br}}{k^2(2\pi)^3} \sum_s \int_0^\infty dp p^2 n_F(p) \times [1 - n_F(p - k)] \theta(p - k) \frac{dP_{q \rightarrow \gamma q}^s(\mathbf{p}, \mathbf{k})}{dkdL}, \quad (2)$$

where $d_{br} = 4N_c$ is the number of the quark and antiquark states,

$$n_F(p) = \frac{1}{\exp(p/T) + 1} \quad (3)$$

is the thermal Fermi distribution, and $dP_{q \rightarrow \gamma q}^s(\mathbf{p}, \mathbf{k})/dkdL$ is the photon emission probability distribution per unit length for a quark of type s . In the small angle approximation we can take the vectors \mathbf{p} and \mathbf{k} parallel. The annihilation contribution can be expressed via the probability distribution for the photon absorption with the help of the detailed balance principle. It leads to the formula [30]

$$\frac{dN_{an}}{dtdVd\mathbf{k}} = \frac{d_{an}}{(2\pi)^3} \sum_s \int_0^\infty dp n_F(p) \times n_F(k - p) \theta(k - p) \frac{dP_{\gamma \rightarrow q\bar{q}}^s(\mathbf{k}, \mathbf{p})}{dpdL}, \quad (4)$$

where $d_{an} = 2$ is the number of the photon helicities, $dP_{\gamma \rightarrow q\bar{q}}^s(\mathbf{k}, \mathbf{p})/dpdL$ is the probability distribution per unit length for the $\gamma \rightarrow q\bar{q}$ transition (p is the quark momentum and $k - p$ is the antiquark momentum, and similarly to $q \rightarrow \gamma q$ we can take the vectors \mathbf{p} and \mathbf{k} parallel).

In the LCPI formalism [22] the probability of the $q \rightarrow \gamma q$ transition per unit length (in terms of the fractional photon momentum $x = k/p$) can be written as

$$\frac{dP_{q \rightarrow \gamma q}}{dxdL} = 2\text{Re} \int_0^\infty dz \exp\left(-i\frac{z}{L_f}\right) \hat{g}(x) \times [\mathcal{K}(\boldsymbol{\rho}_2, z|\boldsymbol{\rho}_1, 0) - \mathcal{K}_{vac}(\boldsymbol{\rho}_2, z|\boldsymbol{\rho}_1, 0)] \Big|_{\boldsymbol{\rho}_{1,2}=0}, \quad (5)$$

where $L_f = 2M(x)/\epsilon^2$ with $M(x) = E_q x(1 - x)$, $\epsilon^2 = m_q^2 x^2 + m_\gamma^2 (1 - x)$ (in general for $a \rightarrow b + c$ transition $\epsilon^2 = m_b^2 x_c + m_c^2 x_b - m_a^2 x_b x_c$), \hat{g} is the vertex operator, given by

$$\hat{g}(x) = \frac{V(x)}{M^2(x)} \frac{\partial}{\partial \boldsymbol{\rho}_1} \cdot \frac{\partial}{\partial \boldsymbol{\rho}_2} \quad (6)$$

with

$$V(x) = z_q^2 \alpha_{em} (1 - x + x^2/2)/x, \quad (7)$$

$\alpha_{em} = e^2/4\pi$ the fine-structure constant. In (5) \mathcal{K} is the retarded Green's function of a two dimensional Schrödinger equation with the Hamiltonian

$$\hat{\mathcal{H}} = -\frac{1}{2M(x)} \left(\frac{\partial}{\partial \boldsymbol{\rho}} \right)^2 + v(\boldsymbol{\rho}), \quad (8)$$

and \mathcal{K}_{vac} is the Green function for $v = 0$. The potential v can be written as

$$v = -iP(x\rho), \quad (9)$$

where the function $P(\rho)$ describes interaction of the color singlet $q\bar{q}$ dipole with the QGP. In the HTL scheme with static coupling constant g $P(\rho)$ can be written as [30, 31]

$$P(|\rho|) = \frac{g^2 C_F T}{(2\pi)^2} \int d\mathbf{q}_\perp [1 - \exp(i\rho\mathbf{q}_\perp)] C(\mathbf{q}_\perp), \quad (10)$$

$$C(\mathbf{q}_\perp) = \frac{m_D^2}{\mathbf{q}_\perp^2(\mathbf{q}_\perp^2 + m_D^2)}, \quad (11)$$

where $C_F = 4/3$ is the quark Casimir, $m_D = gT[(N_c + N_F/2)/3]^{1/2}$ is the Debye mass. In the approximation of static color Debye-screened scattering centers [20] the function $P(\rho)$ reads

$$P(\rho) = \frac{n\sigma(\rho)}{2}, \quad (12)$$

where n is the number density of the color centers, and $\sigma(\rho)$ is the well known dipole cross section. For running α_s the dipole cross section reads [32]

$$\sigma(|\rho|) = C_T C_F \int d\mathbf{q}_\perp \alpha_s^2(q_T^2) \frac{[1 - \exp(i\mathbf{q}_\perp \rho)]}{(\mathbf{q}_\perp^2 + m_D^2)^2}, \quad (13)$$

where C_T is the color center Casimir. The dipole form (12) was used in our previous jet quenching analyses [4, 25] with $\alpha_s(q^2)$ frozen at some value α_s^{fr} at low momenta.

For numerical calculations it is convenient to use the representation of the spectrum as a sum of the Bethe-Heitler term and an absorptive correction due to higher order rescatterings (describing the Landau-Pomeranchuk-Migdal suppression [23])

$$\frac{dP_{q \rightarrow \gamma q}}{dxdL} = \frac{dP_{q \rightarrow \gamma q}^{BH}}{dxdL} + \frac{dP_{q \rightarrow \gamma q}^{abs}}{dxdL}. \quad (14)$$

It can be derived by expanding the Green's function \mathcal{K} in (5) in a series in the potential v (see [33] for details). The Bethe-Heitler contribution corresponds to the term linear in v . It can be written as

$$\frac{dP_{q \rightarrow \gamma q}^{BH}}{dxdL} = \frac{n}{2} \sum_{\{\lambda\}} \int d\rho |\Psi(x, \rho, \{\lambda\})|^2 \sigma(\rho x), \quad (15)$$

where $\{\lambda\} = (\lambda_q, \lambda_{q'}, \lambda_\gamma)$ is the set of helicities, $\Psi(x, \rho, \{\lambda\})$ is the light-cone wave function for $q \rightarrow \gamma q$ transition with $\lambda_{q'} = \lambda_q$. The contribution of the higher order rescatterings reads

$$\frac{dP_{q \rightarrow \gamma q}^{abs}}{dxdL} = -\frac{n^2}{4} \text{Re} \sum_{\{\lambda\}} \int_0^\infty dz \int d\rho \Psi^*(x, \rho, \{\lambda\}) \times \sigma(\rho x) \Phi(x, \rho, \{\lambda\}, z, 0) \exp\left(-\frac{iz}{L_f}\right), \quad (16)$$

where

$$\Phi(x, \rho, \{\lambda\}, z_2, z_1) = \int d\rho' \mathcal{K}(\rho, z_2 | \rho', z_1) \times \Psi(x, \rho', \{\lambda\}) \sigma(\rho' x) \quad (17)$$

is the solution of the Schrödinger equation with the boundary condition $\Phi(x, \rho, \{\lambda\}, z_1, z_1) = \Psi(x, \rho, \{\lambda\}) \sigma(\rho x)$.

For $\gamma \rightarrow q\bar{q}$ one can obtain similar formulas. But now $M(x) = E_\gamma x(1-x)$ (x is the quark fractional momentum) $\epsilon^2 = m_q^2 - m_\gamma^2 x(1-x)$, and

$$V(x) = z_q^2 \alpha_{em} N_c [x^2 + (1-x)^2]/2. \quad (18)$$

The formulas for the light-cone wave functions for the $q \rightarrow \gamma q$ and $\gamma \rightarrow q\bar{q}$ are similar to that that for the QED processes $e \rightarrow \gamma e$ and $\gamma \rightarrow e\bar{e}$ given in [23].

We will present the results for two versions of the model: for the phenomenological scenario with running α_s and for the pQCD HTL scenario with static coupling [17]. For the scenario with running coupling, as in our jet quenching analyses, we use the dipole formulas (12), (13). In jet quenching analyses [4, 25] we used the quark quasiparticle mass $m_q = 300$ MeV. For the relevant temperature region $T \sim (1-3)T_c$, it is supported by the analysis of Ref. [26] of the lattice data in the quasiparticle model. For the induced gluon emission the results are practically insensitive to the light quark mass. But for the photon emission the value of the quark mass is important. As was shown recently in Ref. [27], in a strongly coupled QGP the thermal quark mass may be much smaller than the pQCD prediction based on the HTL scheme. Therefore, for the phenomenological scenario we present the results for two very different values of the thermal quark mass: $m_q = 300$ MeV (as obtained in Ref. [26]) and $m_q = 50$ MeV. The latter value is much smaller than the thermal pQCD HTL quark mass, and the results should be close to that for the massless quarks supported by the analysis [27]. As in jet quenching analyses, for the version with running α_s we use the Debye mass obtained in the lattice calculations [34], that give m_D/T slowly decreasing with T ($m_D/T \approx 3$ at $T \sim 1.5T_c$, $m_D/T \approx 2.4$ at $T \sim 4T_c$). For the pQCD HTL scenario we use for the quark and Debye masses the standard pQCD values ($m_q = gT/\sqrt{3}$, $m_D = gT[(N_c + N_F/2)/3]^{1/2}$), and the formulas (10), (11) for the function $P(\rho)$. To account for the mass suppression for strange quarks we take $N_f = 2.5$ as in our jet quenching analyses [4].

III. NUMERICAL RESULTS FOR PHOTON SPECTRUM IN AA COLLISIONS

In calculating the photon spectrum in AA collisions we perform the four volume integration using the proper time τ and rapidity Y variables

$$\tau = \sqrt{t^2 - z^2}, \quad Y = \frac{1}{2} \ln \left(\frac{t+z}{t-z} \right). \quad (19)$$

In these coordinates the photon spectrum reads

$$\frac{dN}{dyd\mathbf{k}_T} = \int \tau d\tau dY d\boldsymbol{\rho} \omega' \frac{dN(T', k')}{dt' dV' d\mathbf{k}'}, \quad (20)$$

where primed quantities correspond to the comoving frame, and $\omega' = k' = |\mathbf{k}'|$.

We describe the plasma fireball at $\tau > \tau_0$ in the Bjorken model [35] without the transverse expansion that gives the entropy density $s \propto 1/\tau$. We present the results for the ideal gas model (with the temperature dependence of the entropy density $s \propto T^3$), that gives $T = T_0(\tau_0/\tau)^{1/3}$ in the plasma phase. We also perform calculations for the temperature dependence of the entropy density $s(T)$ obtained in the lattice simulation [36]. As in jet quenching analyses [4] we take $\tau_0 = 0.5$ fm. To account for qualitatively the fact that the process of the QGP production is not instantaneous, we take the entropy density $\propto \tau$ in the interval $0 < \tau < \tau_0$. However, the contribution of this region is relatively small. We calculate the initial density profile of the QGP fireball at the proper time τ_0 assuming that the initial entropy is proportional to the charged particle pseudorapidity multiplicity density at $\eta = 0$ calculated in the two component wounded nucleon Glauber model [37] (the details and model parameters can be found in [11, 38]). In the space-time integral (20) we drop the points with $T_0 < T_c$ (here $T_c = 160$ MeV is the deconfinement temperature) at $\tau = \tau_0$. For the ideal gas model we treat the crossover region at $T \sim T_c$ as a mixed phase, and take the entropy density in this phase $\propto 1/\tau$ [35]. In the mixed phase we account for the photon emission only from the QGP phase. Note that contribution of the space-time region with $T \sim T_c$ to the photon spectrum (both for the ideal gas fireball model and for the lattice version of the entropy density) is relatively small at $k_T \gtrsim 1.5 - 2$ GeV.

For the phenomenological scenario with running QCD coupling we assume that at low momenta α_s is frozen at the value $\alpha_s^{fr} = 0.5$, that is supported by our jet quenching analyses of the nuclear modification factors R_{AA} [4] and I_{AA} [39] in Au+Au collisions at $\sqrt{s} = 0.2$ TeV. For the HTL scenario with fixed coupling we take $\alpha_s = 0.3$. In Fig. 1 we show our results for the ideal gas model of the QGP for the photon spectrum $dN/dydk_T = (1/2\pi k_T) dN/dydk_T$ (averaged over the azimuthal angle) for Au+Au collisions at $\sqrt{s} = 0.2$ TeV for 0–20% centrality bin for the phenomenological scenario with running coupling for $m_q = 300$ and 50 MeV and for the HTL scenario. We compare our results with the data from PHENIX [8]. The theoretical curves have been obtained integrating in (20) up to $\tau_{max} = 10$ fm. At $k_T \gtrsim 1$ GeV the photon spectrum is only weakly sensitive to τ_{max} . It occurs because the main contribution at $k_T \gg T_0$ comes from the hottest space-time region of the QGP with τ up to several units of τ_0 . For $\tau_{max} = R_A \approx 6.4$ fm the photon spectrum at $k_T \sim 1$ GeV is reduced only by $\sim 10\%$ and for $k_T \gtrsim 2$ GeV the change in the spectrum is negligible. For the HTL scenario we also present in Fig. 1 the sum of the contributions from the collinear processes and

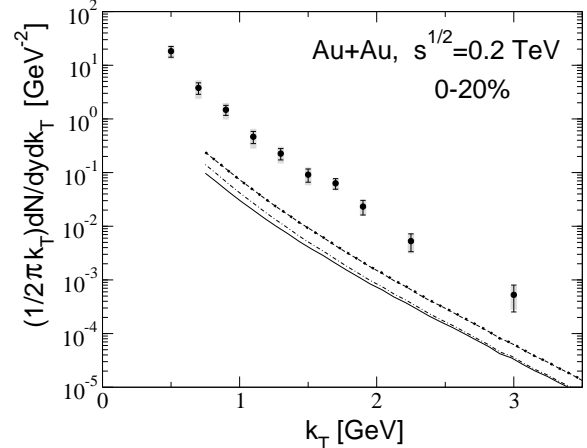


FIG. 1: The photon spectrum $(1/2\pi k_T) dN/dydk_T$ averaged over the azimuthal angle for Au+Au collisions at $\sqrt{s} = 0.2$ TeV in the 0–20% centrality range. Solid: the sum of the $q \rightarrow \gamma q$ and $q\bar{q} \rightarrow \gamma$ processes for running coupling with $\alpha_s^{fr} = 0.5$ for $m_q = 300$ MeV, dotted: the same as solid but for $m_q = 50$ MeV, dot-dashed: the sum of the $q \rightarrow \gamma q$ and $q\bar{q} \rightarrow \gamma$ processes for the HTL scheme for $\alpha_s = 0.3$, dashed: the sum of the collinear process with the LO $2 \rightarrow 2$ processes for the HTL scheme for $\alpha_s = 0.3$. The theoretical curves are for the ideal gas model for $\tau_0 = 0.5$ fm. Data points are from

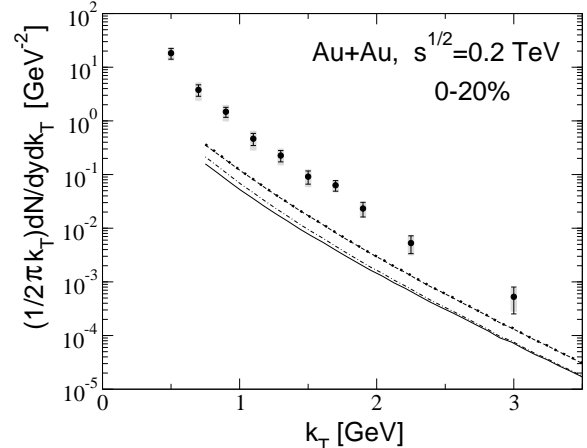


FIG. 2: Same as in Fig. 1 but for calculations with the entropy density $s(T)$ from the lattice simulation [36].

from the LO contribution due to $2 \rightarrow 2$ processes in the form obtained in [17]. From Fig. 1 one can see that the results for the phenomenological scenario with running coupling and $m_q = 300$ MeV are close to that for the HTL scenario with fixed coupling. But for the phenomenological scenario with $m_q = 50$ MeV the photon spectrum is bigger than that for the HTL scenario by a factor of ~ 2 . Note that the photon yields obtained for $m_q = 300$ and 50 MeV do not follow the power law $1/m_q^2$. This is due to the Landau-Pomeranchuk-Migdal suppression, described

by the absorptive term on the right-hand side of (14), that becomes very strong for small m_q . In this regime the quark mass dependence becomes very weak. Our calculations show that the photon spectrum for $m_q = 100$ MeV is smaller than that for $m_q = 50$ MeV only by $\sim 20\%$. From Fig. 1 one can see that at $k_T \gtrsim 1.5 - 2$ GeV for the HTL scenario the theoretical curves for the sum of the contribution from the collinear processes $q \rightarrow \gamma q$ and $q\bar{q}\gamma$ and the LO mechanisms underpredict the data typically by a factor of $\sim 5 - 7$. Assuming that for the phenomenological scenario the relative effect of the $2 \rightarrow 2$ processes is similar to that for the HTL scenario ¹, we can conclude that even for the version with $m_q = 50$ MeV the experimental spectrum will be underestimated by a factor of ~ 3 . The situation becomes better for the results obtained for the lattice temperature dependence of the entropy density, that are shown in Fig. 2. In this case the theoretical predictions are approximately increased by a factor of $\sim 1.5 - 2$, and the disagreement with the data becomes smaller. The inclusion of the hadron gas phase [40] can improve the agreement with the data at low k_T ($k_T \lesssim 1$ GeV). But it cannot increase significantly the photon spectrum at $k_T \sim 2 - 3$ GeV. Thus, we can conclude that in this high- k_T region, even for the scenario with a small thermal quark mass, one cannot avoid some underestimation of the photon spectrum.

The agreement with the data at high k_T can be improved for a smaller value of the thermalization time τ_0 . Our calculations for $\tau_0 = 0.25$ fm show that the theoretical predictions increase by a factor of ~ 2 at $k_T \sim 2 - 3$ GeV. However, such a small value of τ_0 does not seem realistic, because it is of the order of the inverse saturation scale $1/Q_s$ ($Q_s \sim 1 - 1.5$ GeV for RHIC conditions [41]). And in this time region the description in terms of the pre-equilibrium plasma stage is more appropriate. The considerable increase of the photon spectrum for $\tau_0 = 0.25$ fm can be viewed as an indication that the plasma phase contribution to the photon production at $k_T \gtrsim 2$ GeV can be large. In fact, the plasma effect can be considerably bigger. Because the typical Lorentz force that quarks undergo in the plasma is by a factor of $\sim 10 - 20$ bigger than that for the Debye screened color

centers in the thermalized QGP [42]. However, due to finite formation length of the collinear photon emission an accurate analysis of the collinear processes including the pre-equilibrium plasma stage is a complicated task. Because, due to the nonlocal nature the photon emission, the photon spectrum should be sensitive to the whole process of the QGP formation, and one simply cannot distinguish the photon emission from the plasma and from the QGP at $\tau \sim \tau_0$. It is worth to note that the magnitude of the jet quenching is not strongly affected by the variation of τ_0 from ~ 0.5 fm to ~ 0.25 . It is due to a strong reduction of the radiative parton energy loss by the finite size effects for the first fm/c of the matter evolution [43]. For the same reason the plasma effect on jet quenching also turns out to be small [42].

IV. SUMMARY

We have studied the role of running coupling and the effect of variation of the thermal quark mass on contribution of the collinear processes $q \rightarrow \gamma q$ and $q\bar{q} \rightarrow \gamma$ in the QGP phase to the photon spectrum in AA collisions in a phenomenological scheme similar to that used in our previous successful jet quenching analyses based on the LCPI approach [22] to the induced gluon emission. The analysis of the collinear photon emission is also performed within the LCPI formalism [22]. We reduce calculation of the photon emission rate to solving a two dimensional Schrödinger equation. For the pQCD model with static coupling constant and the thermal quark mass predicted by the HTL scheme our method is equivalent to the well known AMY formalism [17]. We found that for the model of the QGP evolution that allows one to obtain a reasonable description of jet quenching both the models for the photon emission underestimate considerably the photon spectrum measured by PHENIX [8]. For the phenomenological scenario with running α_s with a very small thermal quark mass ($m_q = 50$ MeV) the contribution of the higher order collinear processes summed with the LO $2 \rightarrow 2$ processes can explain $\sim 50\%$ of the experimental photon yield from PHENIX [8] at $k_T \sim 2 - 3$ GeV. Thus, we conclude that, for the picture of the QGP evolution and for the model of multiple parton scattering in the QGP consistent with data on jet quenching, the photon emission from the QGP stage alone is not enough to fit the data on the photon production in $Au+Au$ collisions at $k_T \sim 2 - 3$ GeV even for the scenario with a very small thermal quark mass.

¹ The incorporation of running α_s for the $2 \rightarrow 2$ processes was not elaborated yet. However, calculations in the HTL scheme with static α_s show that contribution of the LO processes has relatively low sensitivity to α_s (say, for $\alpha_s = 0.3$ the growth of the LO contribution as compared to that for $\alpha_s = 0.2$ is $\lesssim 10 - 25\%$). Therefore, the effect of running coupling constant on the $2 \rightarrow 2$ processes should not be very large. Note that even for the scenario with a very small thermal quark mass [27] the contribution of the $2 \rightarrow 2$ processes should not change significantly. Because it depends logarithmically on the quark quasiparticle mass. And even for a vanishing quasiparticle mass in an infinite QGP, for the $2 \rightarrow 2$ process in the expanding QGP the effective quark virtuality cannot be much smaller than $1/\tau_{ev}$, where $\tau_{ev} \sim 1 - 4$ fm is the typical QGP evolution time dominating the photon emission.

Acknowledgments

This work has been supported by the RScF grant 16-12-10151.

References

[1] J.-P. Blaizot, F. Gelis, J.-F. Liao, L. McLerran, and R. Venugopalan, Nucl. Phys. **A873**, 68 (2012) [arXiv:1107.5296].

[2] I.M. Dremin and A.V. Leonidov, Phys. Usp. **53**, 1123 (2011) [arXiv:1006.4603].

[3] E.V. Shuryak, Phys. Lett. **B78**, 150 (1978).

[4] B.G. Zakharov, JETP Lett. **93**, 683 (2011) [arXiv:1105.2028]; *ibid.* **96**, 616 (2013) [arXiv:1210.4148]; J. Phys. **G40**, 085003 (2013) [arXiv:1304.5742]; *ibid.* **G41**, 075008 (2014) [arXiv:1311.1159].

[5] K.C. Zapp, F. Krauss, and U.A. Wiedemann, JHEP **1303**, 080 (2013) [arXiv:1212.1599].

[6] J. Xu, A. Buzzatti, and M. Gyulassy, JHEP **1408**, 063 (2014) [arXiv:1402.2956].

[7] J.-F. Paquet *et al.*, Phys. Rev. **C93**, 044906 (2016) [arXiv:1509.06738].

[8] A. Adare *et al.* [PHENIX Collaboration], Phys. Rev. **C91**, 064904 (2015) [arXiv:1405.3940].

[9] G. Basar, D. Kharzeev, and V. Skokov, Phys. Rev. Lett. **109**, 202303 (2012) [arXiv:1206.1334].

[10] K. Tuchin, Phys. Rev. **C91**, 014902 (2015) [arXiv:1406.5097].

[11] B.G. Zakharov, Eur. Phys. J. **C76**, 109 (2016) [arXiv:1609.04324].

[12] B.G. Zakharov, Phys. Lett. **B737**, 262 (2014) [arXiv:1404.5047].

[13] V.V. Goloviznin, A.M. Snigirev, and G.M. Zinovjev, JETP Lett. **98**, 61 (2013) [arXiv:1209.2380].

[14] M. Chiu, T.K. Hemmick, V. Khachatryan, A. Leonidov, J. Liao, and L. McLerran, Nucl. Phys. **A900**, 16 (2013) [arXiv:1202.3679].

[15] I. Dremin, M. Kirakosyan, and A. Leonidov, Adv. High Energy Phys. **2013**, 706521 (2013) [arXiv:1305.3812].

[16] J. Berges, K. Reygers, N. Tanji, and R. Venugopalan, Phys. Rev. **C95**, 054904 (2017) [arXiv:1701.05064].

[17] P.B. Arnold, G.D. Moore, and L.G. Yaffe, JHEP **0112**, 009 (2001) [hep-ph/0111107].

[18] P. Aurenche, F. Gelis, and H. Zaraket, Phys. Rev. **D61**, 116001 (2000) [hep-ph/9911367].

[19] B.G. Zakharov, JETP Lett. **80**, 1 (2004) [hep-ph/0405101].

[20] M. Gyulassy and X.N. Wang, Nucl. Phys. **B420**, 583 (1994) [nucl-th/9306003].

[21] R. Baier, Y.L. Dokshitzer, A.H. Mueller, S. Peigné, and D. Schiff, Nucl. Phys. **B483**, 291 (1997) [hep-ph/9607355]; *ibid.* **B484**, 265 (1997) [hep-ph/9608322].

[22] B.G. Zakharov, JETP Lett. **63**, 952 (1996) [hep-ph/9607440]; *ibid.* **65**, 615 (1997) [hep-ph/9704255]; **70**, 176 (1999) [hep-ph/9906536].

[23] B.G. Zakharov, Phys. Atom. Nucl. **61**, 838 (1998) [hep-ph/9807540].

[24] B.G. Zakharov, JETP Lett. **86**, 444 (2007) [arXiv:0708.0816].

[25] B.G. Zakharov, JETP Lett. **88**, 781 (2008) [arXiv:0811.0445].

[26] P. Lévai and U. Heinz, Phys. Rev. **C57**, 1879 (1998) [hep-ph/9710463].

[27] H. Nakagawa, H. Yokota, and K. Yoshida, Phys. Rev. **D85**, 031902 (2012) [arXiv:1111.0117]; Phys. Rev. **D86**, 096007 (2012) [arXiv:1208.6386].

[28] O. Kaczmarek, F. Karsch, M. Kitazawa, and W. Soldner, Phys. Rev. **D86**, 036006 (2012) [arXiv:1206.1991].

[29] A. Cucchieri, F. Karsch, and P. Petreczky, Phys. Lett. **B497**, 80 (2001) [hep-lat/0004027].

[30] P. Aurenche and B.G. Zakharov, JETP Lett. **85**, 149 (2007) [hep-ph/0612343].

[31] P. Aurenche, F. Gelis, and H. Zaraket, JHEP **0205**, 043 (2002) [hep-ph/0204146].

[32] N.N. Nikolaev and B.G. Zakharov, Z. Phys. **C49**, 607 (1991); *ibid.* **C53**, 331 (1992).

[33] B.G. Zakharov, JETP Lett. **64**, 781 (1996) [hep-ph/9612431].

[34] O. Kaczmarek and F. Zantow, Phys. Rev. **D71**, 114510 (2005) [hep-lat/0503017].

[35] J.D. Bjorken, Phys. Rev. **D27**, 140 (1983).

[36] S. Borsanyi *et al.*, JHEP **1011**, 077 (2010) [arXiv:1007.2580].

[37] D. Kharzeev and M. Nardi, Phys. Lett. **B507**, 121 (2001) [nucl-th/0012025].

[38] B.G. Zakharov, JETP Lett. **104**, 6 (2016) [arXiv:1605.06012].

[39] B.G. Zakharov, JETP in press [arXiv:1706.03980].

[40] S. Turbide, R. Rapp, and C. Gale, Phys. Rev. **C69**, 014903 (2004) [hep-ph/0308085].

[41] T. Lappi, Eur. Phys. J. **C71**, 1699 (2011) [arXiv:1104.3725].

[42] P. Aurenche and B.G. Zakharov, Phys. Lett. **B718**, 937 (2013) [arXiv:1205.6462].

[43] B.G. Zakharov, JETP Lett. **73**, 49 (2001) [hep-ph/0012360].